

This article was downloaded by:

On: 23 January 2011

Access details: *Access Details: Free Access*

Publisher *Taylor & Francis*

Informa Ltd Registered in England and Wales Registered Number: 1072954 Registered office: Mortimer House, 37-41 Mortimer Street, London W1T 3JH, UK



## Journal of Coordination Chemistry

Publication details, including instructions for authors and subscription information:

<http://www.informaworld.com/smpp/title~content=t713455674>

### Hydrothermal syntheses, crystal structures and luminescence properties of two lanthanide dinuclear complexes with hexafluoroglutarate

Yanbin Zhang<sup>a</sup>; Xia Li<sup>a</sup>; Yanqiu Li<sup>a</sup>

<sup>a</sup> Department of Chemistry, Capital Normal University, Beijing 100037, China

First published on: 01 October 2010

**To cite this Article** Zhang, Yanbin , Li, Xia and Li, Yanqiu(2009) 'Hydrothermal syntheses, crystal structures and luminescence properties of two lanthanide dinuclear complexes with hexafluoroglutarate', *Journal of Coordination Chemistry*, 62: 4, 583 – 592, First published on: 01 October 2010 (iFirst)

**To link to this Article:** DOI: 10.1080/00958970802307856

**URL:** <http://dx.doi.org/10.1080/00958970802307856>

PLEASE SCROLL DOWN FOR ARTICLE

Full terms and conditions of use: <http://www.informaworld.com/terms-and-conditions-of-access.pdf>

This article may be used for research, teaching and private study purposes. Any substantial or systematic reproduction, re-distribution, re-selling, loan or sub-licensing, systematic supply or distribution in any form to anyone is expressly forbidden.

The publisher does not give any warranty express or implied or make any representation that the contents will be complete or accurate or up to date. The accuracy of any instructions, formulae and drug doses should be independently verified with primary sources. The publisher shall not be liable for any loss, actions, claims, proceedings, demand or costs or damages whatsoever or howsoever caused arising directly or indirectly in connection with or arising out of the use of this material.

# Hydrothermal syntheses, crystal structures and luminescence properties of two lanthanide dinuclear complexes with hexafluoroglutarate

YANBIN ZHANG, XIA LI\* and YANQIU LI

Department of Chemistry, Capital Normal University, Beijing 100037, China

(Received 29 January 2008; in final form 9 May 2008)

Two complexes  $[\text{Ln}_2(\text{hfga})_2(\text{phen})_4(\text{H}_2\text{O})_6] \cdot \text{hfga} \cdot 2\text{H}_2\text{O}$  ( $\text{H}_2\text{hfga}$  = hexafluoroglutaric acid, phen = 1, 10-phenanthroline, Ln=Tb, **1**; Eu, **2**) were synthesized under hydrothermal conditions and their structures determined by X-ray crystallography. The complexes consist of dinuclear units with an inversion center. Each Ln(III) is nine-coordinate with two carboxylate oxygens from two hfga ligands, three oxygens from water and four nitrogens from two phen molecules. Two carboxylate groups of one hfga adopt monodentate coordination to Ln(III) as a long bidentate bridge linking two Ln(III) ions to form a dimer. Ln(III)⋯Ln(III) distances of 9.027(3) Å for **1** and 9.043(3) Å for **2** were observed. Both complexes emit strong fluorescence and show characteristic emission of Tb(III) and Eu(III) ions, respectively.

**Keywords:** Lanthanide; Dinuclear molecule; Hexafluoroglutaric acid; Crystal structure; Fluorescence

## 1. Introduction

The construction of metal-organic coordination polymers is a current interest for fascinating structures and potential applications [1–14]. The combination of various metals with polycarboxylate ligands having rich coordination modes lead to coordination polymers with different shapes and dimensions or with unique properties, resulting in applications such as magnetism, catalysis, adsorption and luminescent probes [4–14]. Many coordination polymers are based on transition metals; design and synthesis of lanthanide-organic coordination polymers are of interest because of high and variable coordination and flexible coordination geometry of lanthanide ions. Lanthanide complexes have unique fluorescence, magnetic properties and potential applications [6–14]. Fluorinated organic ligands improve the luminescence intensity of complexes by reducing the fluorescence quenching of C–H vibrations [15–17]. Hexafluoroglutaric acid ( $\text{H}_2\text{hfga}$ ) is a fully fluorinated aliphatic dicarboxylic acid ligand. Preparation, characterization and a few crystallographic structures of *d*-block metal complexes containing  $\text{H}_2\text{hfga}$  have been reported [18, 19]. However, there have been no systematic studies on lanthanide complexes with  $\text{H}_2\text{hfga}$ . 1,10-Phenanthroline

\*Corresponding author. Email: xiali@mail.cnu.edu.cn

(phen) helps to increase the rigidity and thermal stability of complexes, and can enhance the luminescent properties of lanthanide complexes due to the antenna effect. Therefore, using  $\text{H}_2\text{hfga}$  and phen in hydrothermal reactions of lanthanide nitrate salts give two new compounds with luminescence properties,  $[\text{Ln}_2(\text{hfga})_2(\text{phen})_4(\text{H}_2\text{O})_6] \cdot \text{hfga} \cdot 2\text{H}_2\text{O}$  (Ln=Tb, **1**; Eu, **2**). In this article, we report the preparation, crystal structures, thermal stabilities and luminescent properties of the two complexes.

## 2. Experimental

### 2.1. Materials and physical techniques

All analytical grade reagents and solvents were commercially available and used as received without further purification. The lanthanide(III) nitrates  $\text{Ln}(\text{NO}_3)_3 \cdot 6\text{H}_2\text{O}$  (Ln=Tb, Eu) were prepared by dissolving corresponding lanthanide oxides (99.99%) in nitric acid followed by recrystallization and drying.

Elemental analyses for C, H and N were carried out on an Elementar Vario EL elemental analyzer. The IR spectra were measured with a Bruker Equinox-55 FT-IR spectrometer on KBr disks from 4000–400  $\text{cm}^{-1}$ . The fluorescence spectra of solid state samples were recorded on an F-4500 Fluorescence Spectrophotometer at room temperature. Thermogravimetric analyses were performed on a WCT-1A Thermal Analyzer with a heating rate of 10  $^\circ\text{C min}^{-1}$  from 20 to 1000  $^\circ\text{C}$  in air.

### 2.2. Syntheses of the complexes

A mixture of  $\text{Ln}(\text{NO}_3)_3 \cdot 6\text{H}_2\text{O}$  (0.1359 g, 0.3 mmol) (Ln=Tb and Eu), hexafluoroglutaric acid (0.1080 g, 0.45 mmol), 1,10-phenanthroline (0.1093 g, 0.6 mmol), deionized water (10 mL) and sodium hydroxide aqueous solution (2 mol  $\text{L}^{-1}$ , 0.33 mL) was placed in a 25 mL Teflon-lined stainless steel autoclave; the pH was about 4.5. After stirring, the mixture was sealed and heated at 160  $^\circ\text{C}$  for 4 days under autogenous pressure, then cooled to 100  $^\circ\text{C}$  at a rate of 5  $^\circ\text{C h}^{-1}$ , followed by slow cooling to room temperature. Colorless block-like single crystals suitable for X-ray diffraction were obtained in about 51.4% for **1** and 48.7% for **2** yield (based on Ln). If the amount of NaOH aqueous solution was 0.28 mL (pH about 4.3), clear aqueous solution without precipitate was obtained, and if the amount of NaOH was 0.36 mL (pH about 4.8), only powder was obtained. When the heating temperature was 180  $^\circ\text{C}$  or higher, black powder was obtained, implying that the ligand may decompose at high temperature. When the temperature was lower than 110  $^\circ\text{C}$ , only pellucid solution was obtained, showing that lower temperature is inappropriate to form these complexes. Anal. Calcd (%) for  $\text{C}_{63}\text{H}_{48}\text{Tb}_2\text{F}_{18}\text{N}_8\text{O}_{20}$  (1897.57) (**1**): C, 39.90; H, 2.531; N, 5.906. Found (%): C, 39.76; H, 2.514; N, 5.769. IR data (KBr,  $\nu\text{cm}^{-1}$ ): 3396 br, 1657 vs, 1595 m, 1575 m, 1520 m, 1423 s, 1406 s, 1260 m, 1169 s, 1048 s, 924 m, 846 s, 808 m, 730 s, 417 w. Anal. Calcd (%) for  $\text{C}_{63}\text{H}_{48}\text{Eu}_2\text{F}_{18}\text{N}_8\text{O}_{20}$  (1883.01) (**2**): C, 40.19; H, 2.550; N, 5.949. Found (%): C, 39.93; H, 2.530; N, 5.797. IR data (KBr,  $\nu\text{cm}^{-1}$ ): 3391 br, 1657 vs, 1595 m, 1575 m, 1520 m, 1423 s, 1406 s, 1260 m, 1169 s, 1048 s, 924 m, 847 s, 808 m, 730 s, 417 w.

### 2.3. Crystallographic data collection and structure determination

Single-crystal X-ray diffraction of **1** and **2** were performed on a Bruker SMART diffractometer equipped with a CCD area detector with a graphite monochromator situated in the incident beam for data collection. Determination of unit cell parameters and data collections were performed with Mo-K $\alpha$  radiation ( $\lambda = 0.71073 \text{ \AA}$ ) by  $\omega$  scan mode in the range of  $1.51 \leq \theta \leq 26.47$  for **1** and  $2.33 \leq \theta \leq 25.30$  for **2** at 293(2) K. All data were corrected by semi-empirical method using SADABS [20]. The program SAINT [21] was used for integration of the diffraction profiles. All structures were solved by direct methods using SHELXS of the SHELXTL-97 package and refined with SHELXL [22, 23]. Metal atom centers were located from the E-maps and other non-hydrogen atoms were located in successive difference Fourier syntheses. The final refinements were performed by full matrix least-squares on  $F^2$  with anisotropic thermal parameters for non-hydrogen atoms. All hydrogen atoms were first found in difference electron density maps, and then placed in the calculated sites and included in the final refinement in the riding model approximation with displacement parameters derived from the parent atoms to which they were bonded. The atoms of free hfga have positional disorder. The crystallographic data and structure refinement of the two complexes are summarized in table 1. Selected bond lengths and angles of **1** and **2** are listed in tables 2 and 3, respectively.

Table 1. Crystal data and structure refinement for **1** and **2**.

Complex	<b>1</b>	<b>2</b>
Empirical formula	C <sub>63</sub> H <sub>48</sub> Tb <sub>2</sub> F <sub>18</sub> N <sub>8</sub> O <sub>20</sub>	C <sub>63</sub> H <sub>48</sub> Eu <sub>2</sub> F <sub>18</sub> N <sub>8</sub> O <sub>20</sub>
Formula weight	1897.57	1883.01
Crystal size (mm <sup>3</sup> )	0.20 × 0.16 × 0.12	0.18 × 0.12 × 0.08
Temperature (K)	293(2)	293(2)
Wavelength (Å)	0.71073	0.71073
Crystal system	Monoclinic	Triclinic
Space group	<i>P</i> <sub>2</sub> <sub>1</sub> / <i>c</i>	<i>P</i> <sub>1</sub>
Unit cells and dimensions (Å, °)		
<i>a</i>	9.2889(12)	9.2573(19)
<i>b</i>	18.422(2)	13.425(3)
<i>c</i>	20.856(3)	14.453(3)
$\alpha$		82.60(3)
$\beta$	107.769(5)	74.66(3)
$\gamma$		76.69(3)
<i>V</i> (Å <sup>3</sup> )	3398.6(8)	1681.3(7)
<i>Z</i>	2	1
<i>D</i> <sub>Calcd</sub> (Mg m <sup>-3</sup> )	1.854	1.860
$\mu$ (mm <sup>-1</sup> )	2.194	1.980
<i>F</i> (000)	1868	930
$\theta$ range for data collection (°)	1.51–26.47	2.33–25.30
Limiting indices	–11 ≤ <i>h</i> ≤ 11 –23 ≤ <i>k</i> ≤ 18 –26 ≤ <i>l</i> ≤ 22	–11 ≤ <i>h</i> ≤ 11 –16 ≤ <i>k</i> ≤ 16 –17 ≤ <i>l</i> ≤ 17
Reflections collected/unique	19285/7015 [ <i>R</i> <sub>(int)</sub> = 0.0258]	11516/6120 [ <i>R</i> <sub>(int)</sub> = 0.0428]
Data/restraints/parameters	7015/173/649	6120/26/538
Goodness-of-fit on <i>F</i> <sup>2</sup>	1.076	1.003
Final <i>R</i> indices [ <i>I</i> > 2 $\sigma$ ( <i>I</i> )]	<i>R</i> <sub>1</sub> = 0.0246, <i>wR</i> <sub>2</sub> = 0.0616	<i>R</i> <sub>1</sub> = 0.0665, <i>wR</i> <sub>2</sub> = 0.1607
<i>R</i> indices (all data)	<i>R</i> <sub>1</sub> = 0.0286, <i>wR</i> <sub>2</sub> = 0.0637	<i>R</i> <sub>1</sub> = 0.0713, <i>wR</i> <sub>2</sub> = 0.1638
Largest diff. peak and hole (e <sup>+</sup> Å <sup>-3</sup> )	0.566 and –0.834	0.612 and –0.884

Table 2. Selected bond lengths (Å) and angles (°) for **1**.

Tb(1)–O(3)	2.320(19)	Tb(1)–O(1)	2.340(18)
Tb(1)–O(7)	2.441(19)	Tb(1)–O(5)	2.458(18)
Tb(1)–O(6)	2.477(2)	Tb(1)–N(4)	2.602(2)
Tb(1)–N(2)	2.617(2)	Tb(1)–N(3)	2.662(2)
Tb(1)–N(1)	2.673(2)		
O(3)–Tb(1)–O(1)	90.85(7)	O(3)–Tb(1)–O(7)	140.92(7)
O(1)–Tb(1)–O(7)	79.06(7)	O(3)–Tb(1)–O(5)	76.75(7)
O(1)–Tb(1)–O(5)	137.86(7)	O(7)–Tb(1)–O(5)	133.89(7)
O(3)–Tb(1)–O(6)	133.17(7)	O(1)–Tb(1)–O(6)	135.98(7)
O(7)–Tb(1)–O(6)	66.84(6)	O(5)–Tb(1)–O(6)	67.08(6)
O(3)–Tb(1)–N(4)	72.99(7)	O(1)–Tb(1)–N(4)	135.82(7)
O(7)–Tb(1)–N(4)	88.22(7)	O(5)–Tb(1)–N(4)	79.11(7)
O(6)–Tb(1)–N(4)	71.83(7)	O(3)–Tb(1)–N(2)	136.13(7)
O(1)–Tb(1)–N(2)	73.87(7)	O(7)–Tb(1)–N(2)	77.25(7)
O(5)–Tb(1)–N(2)	87.52(7)	O(6)–Tb(1)–N(2)	72.16(7)
O(3)–Tb(1)–N(3)	72.11(7)	O(1)–Tb(1)–N(3)	73.51(7)
O(7)–Tb(1)–N(3)	68.81(7)	O(5)–Tb(1)–N(3)	135.89(7)
O(6)–Tb(1)–N(3)	115.59(7)	O(3)–Tb(1)–N(1)	73.78(7)
O(1)–Tb(1)–N(1)	69.55(7)	O(7)–Tb(1)–N(1)	133.91(7)
O(5)–Tb(1)–N(1)	68.32(7)	O(6)–Tb(1)–N(1)	115.96(7)
N(4)–Tb(1)–N(2)	143.99(8)	N(4)–Tb(1)–N(3)	62.48(7)
N(2)–Tb(1)–N(3)	136.40(7)	N(4)–Tb(1)–N(1)	137.67(7)
N(2)–Tb(1)–N(1)	62.36(7)	N(3)–Tb(1)–N(1)	128.45(7)

Table 3. Selected bond lengths (Å) and angles (°) for **2**.

Eu(1)–O(4)	2.307(8)	Eu(1)–O(1)	2.357(6)
Eu(1)–O(5)	2.439(8)	Eu(1)–O(7)	2.458(7)
Eu(1)–O(6)	2.483(7)	Eu(1)–N(3)	2.610(8)
Eu(1)–N(2)	2.612(9)	Eu(1)–N(4)	2.657(9)
Eu(1)–N(1)	2.665(8)		
O(4)–Eu(1)–O(1)	91.7(3)	O(4)–Eu(1)–O(5)	139.8(3)
O(1)–Eu(1)–O(5)	79.2(3)	O(4)–Eu(1)–O(7)	75.4(3)
O(1)–Eu(1)–O(7)	139.4(3)	O(5)–Eu(1)–O(7)	134.2(3)
O(4)–Eu(1)–O(6)	133.5(3)	O(1)–Eu(1)–O(6)	134.7(3)
O(5)–Eu(1)–O(6)	67.8(3)	O(7)–Eu(1)–O(6)	66.5(2)
O(4)–Eu(1)–N(2)	136.1(3)	O(1)–Eu(1)–N(2)	72.3(3)
O(5)–Eu(1)–N(2)	78.4(3)	O(7)–Eu(1)–N(2)	90.5(3)
O(6)–Eu(1)–N(2)	71.4(3)	O(4)–Eu(1)–N(3)	75.1(3)
O(1)–Eu(1)–N(3)	136.1(3)	O(5)–Eu(1)–N(3)	84.6(3)
O(7)–Eu(1)–N(3)	78.2(3)	O(6)–Eu(1)–N(3)	71.8(3)
O(4)–Eu(1)–N(4)	72.2(3)	O(1)–Eu(1)–N(4)	73.2(3)
O(5)–Eu(1)–N(4)	67.7(3)	O(7)–Eu(1)–N(4)	134.2(3)
O(6)–Eu(1)–N(4)	117.8(3)	O(4)–Eu(1)–N(1)	74.2(3)
O(1)–Eu(1)–N(1)	70.2(3)	O(5)–Eu(1)–N(1)	135.3(3)
O(7)–Eu(1)–N(1)	69.3(3)	O(6)–Eu(1)–N(1)	113.6(3)
N(2)–Eu(1)–N(3)	143.1(3)	N(2)–Eu(1)–N(4)	135.2(3)
N(3)–Eu(1)–N(4)	62.9(3)	N(2)–Eu(1)–N(1)	61.9(3)
N(3)–Eu(1)–N(1)	139.8(3)	N(4)–Eu(1)–N(1)	128.6(3)

### 3. Results and discussion

#### 3.1. Structural description of **1** and **2**

The molecular structure of **1**, shown in figure 1, consists of one [Tb<sub>2</sub>(hfga)<sub>2</sub>(phen)<sub>4</sub>(H<sub>2</sub>O)<sub>6</sub>] core, one free hfga and two free waters. The latter two will not be

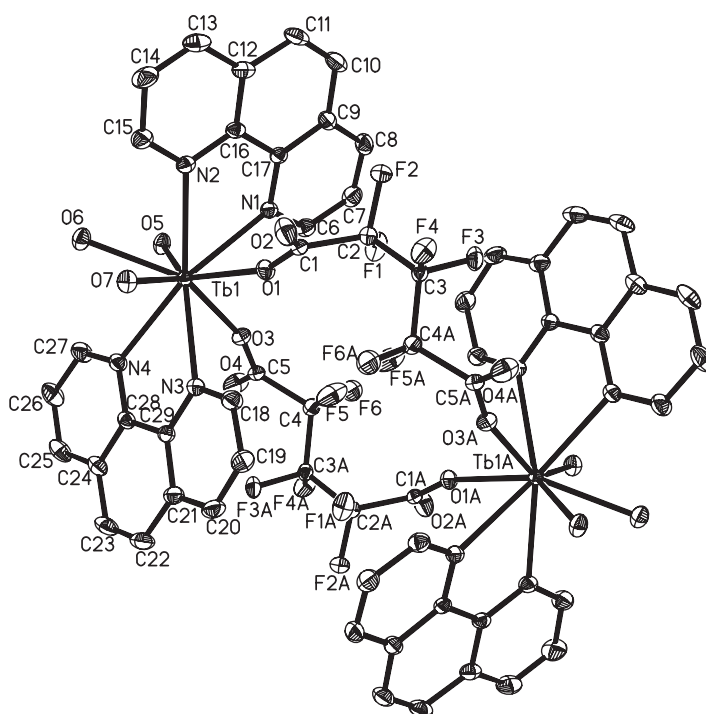


Figure 1. Molecular structure of **1** with thermal ellipsoids at 30% probability. All hydrogen atoms, free water molecules and free hfga are omitted for clarity.

further discussed. The  $[\text{Tb}_2(\text{hfga})_2(\text{phen})_4(\text{H}_2\text{O})_6]$  unit is binuclear with an inversion center. Two Tb(III) ions are linked by doubly bidentate hfga ligands. One monodentate carboxylate oxygen of hfga bonds to a Tb(III), the other monodentate carboxylate oxygen of hfga links another Tb(III). This is rare in lanthanide carboxylate complexes. Many binuclear lanthanide complexes with carboxylate are formed through bidentate-bridging or bridging-chelating  $\text{COO}^-$  groups linking two metal centers, namely,  $\text{Ln}-\text{O}-\text{C}-\text{O}-\text{Ln}$  or  $\text{Ln}-\text{O}-\text{Ln}$ . In **1**, hfga is a long bidentate bridge linking two Tb(III) ions,  $\text{Tb}-\text{OOC}\text{CF}_2\text{CF}_2\text{CF}_2\text{COO}-\text{Tb}$ , resulting in  $\text{Tb}\cdots\text{Tb}$  separation at  $9.027(3)\text{ \AA}$ , larger than in other terbium carboxylate complexes [24]. A large number of lanthanide polycarboxylate complexes have 1-D, 2-D, or 3-D polymeric structures [6–13], and only a few are binuclear [14].

Each Tb(III) is further coordinated to three waters and two phen molecules. The phen chelates the Tb(III) ion to form five-membered rings, blocking polymerization of the binuclear molecule. The dihedral angle between two phen planes is  $85.7^\circ$ , showing that the two phen molecules are approximately vertical, decreasing steric constraints.

The Tb1(III) is nine-coordinate with two carboxylate oxygens (O1 and O3) from two hfga ligands, three oxygens (O5, O6 and O7) from water and four nitrogens (N1, N2, N3 and N4) from two phen molecules. The nine donor atoms around Tb1(III) form a distorted monocapped square antiprism. The bond distances  $\text{Tb1}-\text{O}(\text{carboxyl})$  are  $2.340(18)$  and  $2.320(19)\text{ \AA}$ , respectively, with average bond distance of  $2.330\text{ \AA}$ . The  $\text{Tb1}-\text{O}(\text{water})$  bond distances vary from  $2.441(19)$  to  $2.477(2)\text{ \AA}$  with average

of 2.459 Å. The Tb1–N bond distances are in the range 2.602(2)–2.673(2) Å with average of 2.639 Å. The N2–Tb1–N1 and N4–Tb1–N3 bond angles are 62.36(7)° and 62.48(7)°, respectively.

In the dinuclear molecule, the two bridging hfga ligands and the two Tb(III) centers form a 16-membered loop,  $2[\text{Tb}-\text{OOC}(\text{CF}_2)_2\text{CF}_2\text{COO}-\text{Tb}]$ . Viewed along the *a*-axis, these molecular loops have interesting packing with a channel with a 16-membered loop (A) and big channels (B) observed (figure 2).

Free hfga and two water molecules exist in crystal lattice with strong hydrogen bond interactions between coordinated water and lattice water, between coordinated water and the carboxylate oxygens of uncoordinated hfga and between lattice water and uncoordinated carboxylate oxygens of coordinated hfga. The hydrogen bond distances are in the range 2.641–2.824 Å and the O–H···O angles vary from 110.44–173.22° (table 4). Intermolecular hydrogen bonds between binuclear molecules lead to a 2-D network structure (figure 3) and further consolidate the stability of the structure.

The molecular structure of **2** is shown in figure 4. The structural characteristics of **2** are similar to **1**. So, the details will not be further discussed here. The main difference is in distance between atoms. The Eu1–O (carboxyl) bond distances are 2.307(8) and

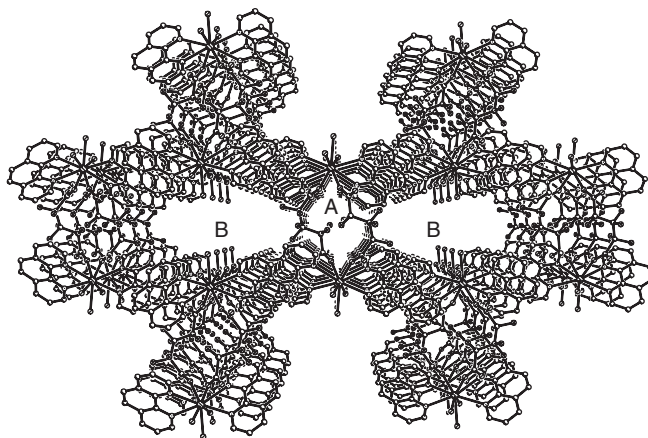


Figure 2. Packing diagram of **1** along the *a*-axis showing channels (A and B). All hydrogen atoms, free water molecules and free hfga are omitted for clarity.

Table 4. Hydrogen bonds (D–H···A) for **1** (Å) and (°).

D–H	<DHA	d(D···A)	A
O5–H5B	110.44	2.738	O10 $[-x+2, -y, -z+1]$
O6–H6A	147.53	2.730	O8 $[x+1, y, z]$
O6–H6A	134.33	2.641	O10 $[-x+2, -y, -z+1]$
O6–H6B	130.90	2.660	O9 $[-x+1, -y, -z+1]$
O6–H6B	140.99	2.775	O11
O7–H7A	123.50	2.752	O12
O7–H7B	114.36	2.824	O11
O12–H12A	170.55	2.753	O4 $[x-1, y, z]$
O12–H12B	173.22	2.724	O2

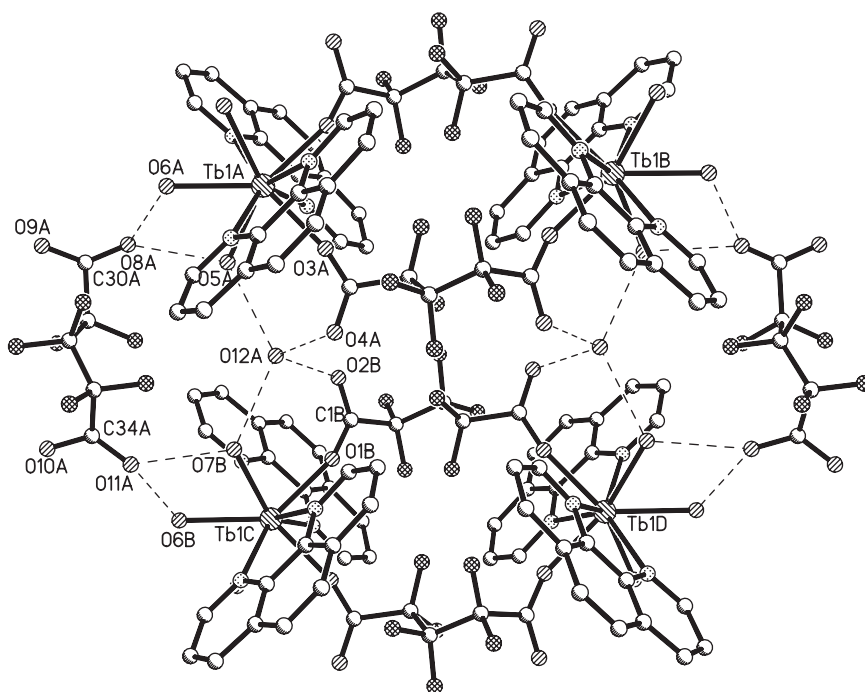


Figure 3. Packing diagram of **1** along the *c*-axis showing 2-D network through H-bonds interactions.

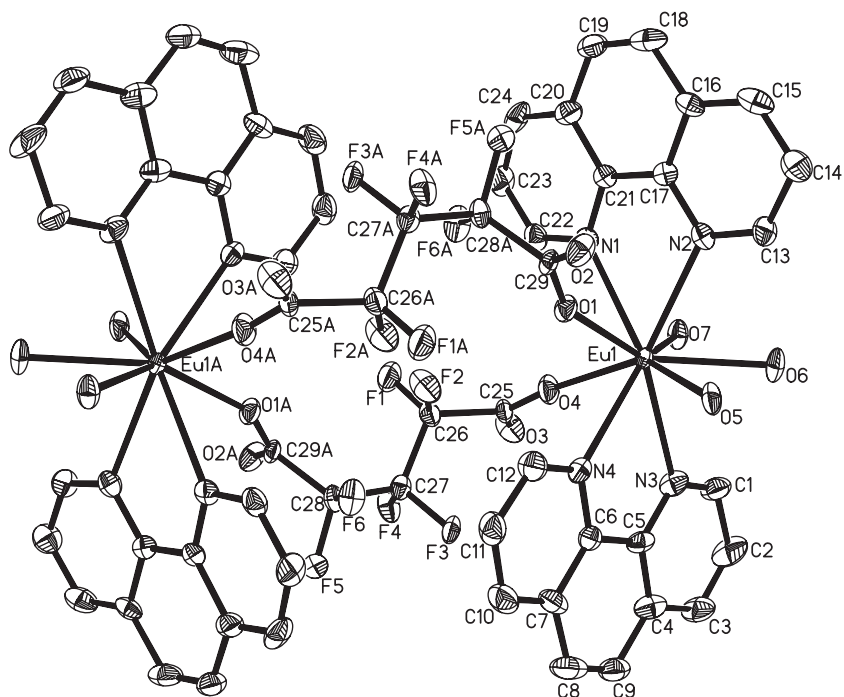


Figure 4. Molecular structure of **2** with thermal ellipsoids at 30% probability. All hydrogen atoms, free water molecules and free hfga are omitted for clarity.



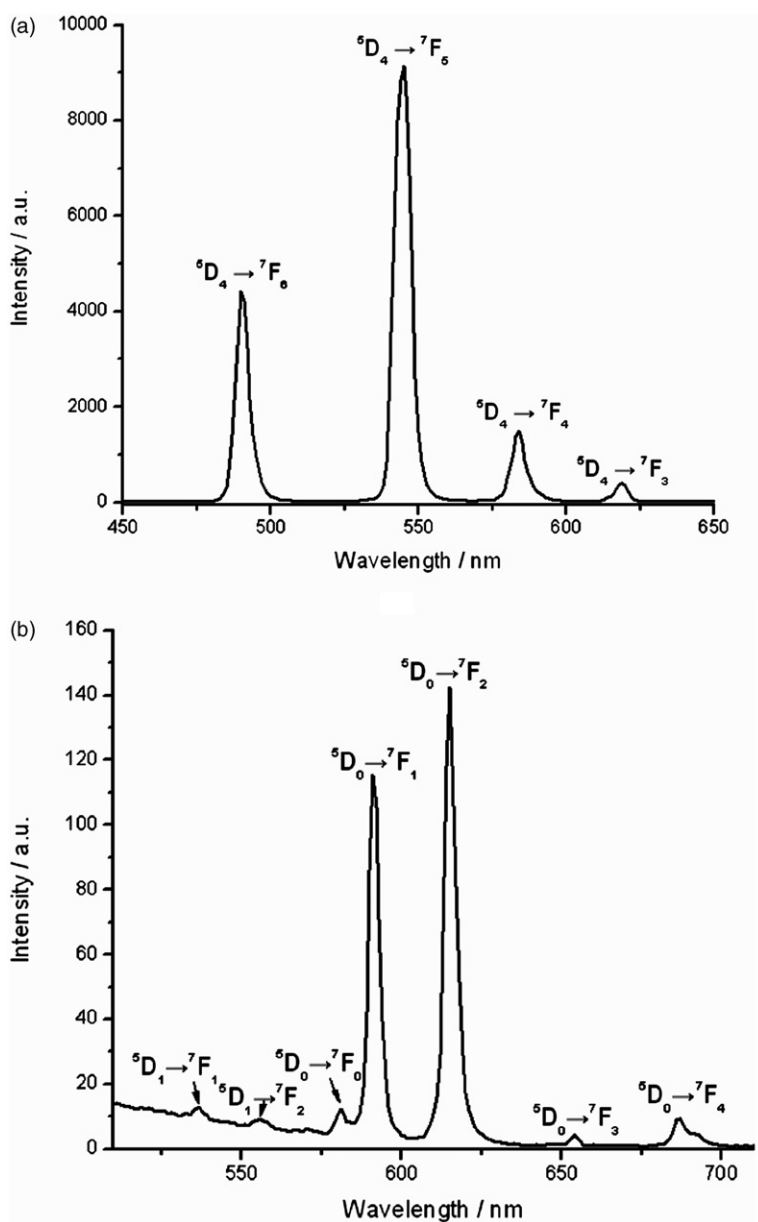


Figure 5. Emission spectra of **1** (a,  $\lambda_{\text{ex}} = 343$  nm) and **2** (b,  $\lambda_{\text{ex}} = 395$  nm).

2.357(6) Å, with average bond distance of 2.332 Å. The Eu1–O (water) distances are in the range 2.439(8)–2.483(7) Å with average of 2.460 Å. The Eu1–N distances are in the range 2.610(8)–2.665(8) Å with average of 2.636 Å. The distance between Eu(III) ions is 9.043(3) Å. The comparison of main crystal data between **2** and **1** shows that the average Eu1–O(carboxyl) distance in **2** is slightly longer than that of Tb1–O(carboxyl) in **1**. The distance between two Eu(III) ions in **2** is longer than that of two Tb(III) ions in **1**. The reason for these differences is the radius of Eu(III) is larger than Tb(III).

### 3.2. Fluorescence spectra

Complexes **1** and **2** emit strong green and red fluorescence, respectively, under ultraviolet light. The fluorescence properties of **1** and **2** in the solid state were investigated at room temperature and their emission spectra were recorded upon excitation at 343 and 395 nm, respectively (figure 5). For **1**, four emission peaks are clearly shown in the emission spectrum at 491, 545, 584 and 619 nm, arising from emitting level ( $^5D_4$ ) to the ground multiplet ( $^7F_{6-3}$ ) of Tb(III),  $^5D_4 \rightarrow ^7F_6$ ,  $^5D_4 \rightarrow ^7F_5$ ,  $^5D_4 \rightarrow ^7F_4$  and  $^5D_4 \rightarrow ^7F_3$  [figure 5(a)]. The most intense emission at 545 nm ( $^5D_4 \rightarrow ^7F_5$ ) is a magnetic dipole and gives an intense green luminescence. The second intense emission at 491 nm ( $^5D_4 \rightarrow ^7F_6$ ) is an electronic dipole transition. The emission spectrum of **2** principally arises from transitions originating at the  $^5D_0$  level of Eu(III) [figure 5(b)]. The strong emission bands at 591 and 615 nm correspond to  $^5D_0 \rightarrow ^7F_1$  and  $^5D_0 \rightarrow ^7F_2$  transitions of Eu(III), respectively.  $^5D_0 \rightarrow ^7F_2$  belonging to an electric dipole transition is stronger than  $^5D_0 \rightarrow ^7F_1$  belonging to a magnetic dipole transition, resulting in red luminescence of **2**. Less intense emission bands at 581, 654 and 688 nm are attributed to  $^5D_0 \rightarrow ^7F_0$ ,  $^5D_0 \rightarrow ^7F_3$  and  $^5D_0 \rightarrow ^7F_4$  transitions, respectively. In the emission spectrum of **2**, weak bands at 537 and 557 nm belong to the transitions of  $^5D_1 \rightarrow ^7F_1$  and  $^5D_1 \rightarrow ^7F_2$ , respectively. The luminescence investigation for **1** and **2** show that hfga is suitable for sensitization of luminescence of Tb(III) and Eu(III).

### 3.3. Thermogravimetric analysis

The TGA-DTA analyses of **1** and **2** were studied from 25 to 1000°C. The TGA-DTA curves of **1** and **2** are similar, showing that decomposition begins at 116°C for **1** and 117°C for **2**, and complete decomposition is achieved above 468°C for **1** and 477°C for **2**. TGA curves exhibit three steps of weight losses, 8.38, 56.45 and 10.28% for **1**, and 8.77, 59.03 and 8.49% for **2**, respectively. The final residues are Tb<sub>4</sub>O<sub>7</sub> for **1** and Eu<sub>2</sub>O<sub>3</sub> for **2**, respectively. The total observed weight losses of 75.11% for **1** and 76.29% for **2**, respectively, are close to the calculated values of 80.30% for **1** and 81.31% for **2**.

## 4. Conclusion

Hexafluoroglutaric acid (H<sub>2</sub>hfga) and 1,10-phenanthroline (phen) react with nitrate salts of lanthanide(III) giving [Ln<sub>2</sub>(hfga)<sub>2</sub>(phen)<sub>4</sub>(H<sub>2</sub>O)<sub>6</sub>]·hfga·2H<sub>2</sub>O (Ln=Tb, **1**; Eu, **2**). The complexes are binuclear through hfga linking two Ln(III) ions. The hfga ligand adopts the rare  $\eta^1:\eta^1-\mu_2$ -coordination. Emission spectra display characteristic fluorescence of Tb(III) and Eu(III) for **1** and **2**, respectively.

## Acknowledgements

We are grateful to the Natural Science Foundation of Beijing (No. 2073022), the Science and Technology Program, Beijing Municipal Education Commission (KM200510028007) and the Young Mainstay Teachers Foundation of Beijing Municipal Universities.

## References

- [1] B.D. Chandler, D.T. Cramb, G.K.H. Shimizu. *J. Am. Chem. Soc.*, **128**, 10403 (2006).
- [2] I. Kumagai, M. Akita-Tanaka, K. Inoue, M. Kurmoo. *J. Mater. Chem.*, **11**, 2146 (2001).
- [3] A. Figuerola, J. Ribas, D. Casanova, M. Maestro, S. Alvarez, C. Diaz. *Inorg.Chem.*, **44**, 6949 (2005).
- [4] A.G. Wong-Foy, A.J. Matzger, O.M. Yaghi. *J. Am. Chem. Soc.*, **128**, 3494 (2006).
- [5] L. Pan, K.M. Adams, H.E. Hernandez, X. Wang, C. Zheng, Y. Hattori, K. Kaneko. *J. Am. Chem. Soc.*, **125**, 3062 (2003).
- [6] T.M. Reineke, M. Eddaoudi, M. Fehr, D. Kelley, O.M. Yaghi. *J. Am. Chem. Soc.*, **121**, 1651 (1999).
- [7] S.S. Yun, Y.B. Park, J.H. Yeon, E.J. Kim, D. Kim. *J. Coord. Chem.*, **60**, 2703 (2007).
- [8] C.G. Zheng, J. Zhang, Z.F. Chen, Z.J. Guo, R.G. Xiong, X.Z. You. *J. Coord. Chem.*, **55**, 835 (2002).
- [9] E.E.S. Teotonio, G.M. Fett, H.F. Brito, A.C. Trindade, M.C.F.C. Felinto. *Inorg. Chem. Commun.*, **10**, 867 (2007).
- [10] X. Li, T.T. Zhang, Z.Y. Zhang, Y.L. Ju. *J. Coord. Chem.*, **60**, 2721 (2007).
- [11] A.E. Koziol, W. Brzyska, B. Klimek, A. Krol, K. Stepniak. *J. Coord. Chem.*, **21**, 183 (1990).
- [12] C. Daugebonne, N. Kerbellec, K. Bernot, Y. Gréault, A. Deluzet, O. Guillou. *Inorg. Chem.*, **45**, 5399 (2006).
- [13] X.J. Zheng, L.P. Jin, S. Gao, S.Z. Lu. *Inorg. Chem. Commun.*, **8**, 72 (2005).
- [14] B. Yan, Y.S. Song, Z.X. Chen. *J. Mol. Struct.*, **694**, 115 (2004).
- [15] Y. Wada, T. Okubo, M. Ryo, T. Nakazawa, Y. Hasegawa, S. Yanegida. *J. Am. Chem. Soc.*, **122**, 8583 (2000).
- [16] G. Mancino, A.J. Ferguson, A. Beeby, N.J. Long, T.S. Jones. *J. Am. Chem. Soc.*, **127**, 524 (2005).
- [17] B.L. Chen, Y. Yang, F. Zapata, G.D. Qian, Y.S. Luo, J.H. Zhang, E.B. Lobkovsky. *Inorg. Chem.*, **45**, 8882 (2006).
- [18] F.A. Cotton, C.A. Murillo, R.M. Yu. *Inorg. Chim. Acta*, **359**, 4811 (2006).
- [19] S.Q. Liu, H. Konaka, T. Kuroda-Sowa, M. Maekawa, Y. Suenaga, G.L. Ning, M. Munakata. *Inorg. Chim. Acta*, **358**, 919 (2005).
- [20] G.M. Sheldrick. *SADABS, Program for Area Detector Adsorption Correction*, Institute for Inorganic Chemistry, University of Göttingen, Germany (1996).
- [21] Bruker AXS, SAINT Software Reference Manual, Madison, WI (1998).
- [22] G.M. Sheldrick. *Phase Annealing in SHELX-97: Direct Methods for Larger Structures*, *Acta Cryst.*, **A46**, 467 (1990).
- [23] G.M. Sheldrick. *SHELXL-97, Program for the Refinement of Crystal Structures*, University of Göttingen, Germany (1997).
- [24] X. Li, Z.Y. Zhang, Y.Q. Zou. *Eur. J. Inorg. Chem.*, **14**, 2909 (2005).